



(51) International Patent Classification:

B22D 11/115 (2006.01) *B22D 27/02* (2006.01)
B01F 13/08 (2006.01) *F27D 27/00* (2010.01)
B22D 11/12 (2006.01)

(21) International Application Number:

PCT/IL2019/050291

(22) International Filing Date:

14 March 2019 (14.03.2019)

(25) Filing Language:

English

(26) Publication Language:

English

(30) Priority Data:

62/642,617 14 March 2018 (14.03.2018) US

(71) Applicant: **NORD ISRAEL RESEARCH AND DEVELOPMENT LTD.** [IL/IL]; 35/21 Bar Nisan St., 8463335 Beer Sheva (IL).

(72) Inventors: **KAPUSTA, Arkady**; 15/10 Shimshon St., 8447204 Beer Sheva (IL). **HAVKIN, Michael**; 35/21 Bar Nisan St., 8463335 Beer Sheva (IL). **MIKHAILOVICH, Boris**; 3/15 Ben Asher St., 8427502 Beer Sheva (IL). **TILMAN, Boris**; 5A/10 Gordon St., 8429446 Beer Sheva (IL). **KUDRIAVTCEV, Aleksei**; 78 Krasnoe Selo, Golubko St.,

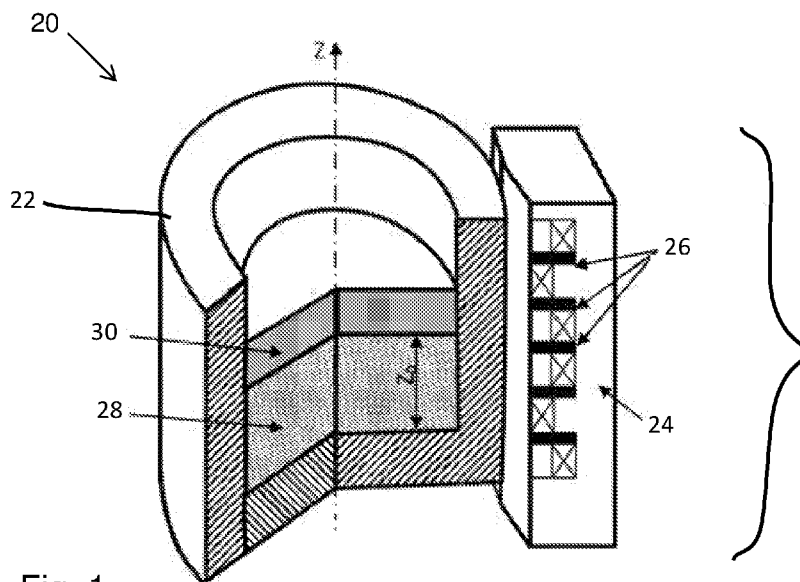
Saint Petersburg, 198320 (RU). **SMIRNOV, Kirill**; 9 Simonov St., Saint Petersburg, 194000 (RU).

(74) Agent: **PAPPER, Vladislav** et al.; Ben-Ami & Associates, P.O Box 94, 7610002 Rehovot (IL).

(81) Designated States (unless otherwise indicated, for every kind of national protection available): AE, AG, AL, AM, AO, AT, AU, AZ, BA, BB, BG, BH, BN, BR, BW, BY, BZ, CA, CH, CL, CN, CO, CR, CU, CZ, DE, DJ, DK, DM, DO, DZ, EC, EE, EG, ES, FI, GB, GD, GE, GH, GM, GT, HN, HR, HU, ID, IL, IN, IR, IS, JO, JP, KE, KG, KH, KN, KP, KR, KW, KZ, LA, LC, LK, LR, LS, LU, LY, MA, MD, ME, MG, MK, MN, MW, MX, MY, MZ, NA, NG, NI, NO, NZ, OM, PA, PE, PG, PH, PL, PT, QA, RO, RS, RU, RW, SA, SC, SD, SE, SG, SK, SL, SM, ST, SV, SY, TH, TJ, TM, TN, TR, TT, TZ, UA, UG, US, UZ, VC, VN, ZA, ZM, ZW.

(84) Designated States (unless otherwise indicated, for every kind of regional protection available): ARIPO (BW, GH, GM, KE, LR, LS, MW, MZ, NA, RW, SD, SL, ST, SZ, TZ, UG, ZM, ZW), Eurasian (AM, AZ, BY, KG, KZ, RU, TJ, TM), European (AL, AT, BE, BG, CH, CY, CZ, DE, DK, EE, ES, FI, FR, GB, GR, HR, HU, IE, IS, IT, LT, LU, LV, MC, MK, MT, NL, NO, PL, PT, RO, RS, SE, SI, SK, SM,

(54) Title: METHOD OF OPTIMIZING ELECTROMAGNETIC STIRRING IN METALLURGICAL TECHNOLOGIES



(57) Abstract: Methods and systems are provided for increasing the efficiency of electromagnetic stirring by applying amplitude-frequency modulation (AFM) of travelling or rotating magnetic fields, where the applied modulation frequency is a resonant frequency that maximizes one or more of: an electromagnetic volume force, a current density, a magnetic induction, a motion velocity of the melt, and an amplitude of vector potential of the melt, or of a mold of the melt.



TR), OAPI (BF, BJ, CF, CG, CI, CM, GA, GN, GQ, GW,
KM, ML, MR, NE, SN, TD, TG).

Published:

— *with international search report (Art. 21(3))*

METHOD OF OPTIMIZING ELECTROMAGNETIC STIRRING IN METALLURGICAL TECHNOLOGIES

RELATED APPLICATION DATA

The present application claims priority from U.S. Provisional Patent Application 62/642,617, filed on March, 14, 2018 and incorporated herein by reference.

FIELD OF THE INVENTION

The present invention is directed to systems and methods of electromagnetic stirring for metallurgical processes.

BACKGROUND OF THE INVENTION

Electromagnetic stirring (EMS) using harmonic rotating or traveling magnetic fields (RMF or TMF) has been used in metallurgy and mechanical engineering in production of ferrous and non-ferrous metals for more than 60 years. The method is widely used on most billet casters and in stationary casting of ingots, in order to improve the macrostructure and chemical homogeneity of ingots and billets, especially for quality steel products.

Experiments on the use of RMF for improving the quality of a continuous cast ingot were performed by E. Pestel [1] and by Junghans and Schaaber [2], who proposed using a three-phase inductor RMF. To increase the efficiency of mixing, they also applied the interruption of current in induction coils with a predetermined period in combination with a change in the direction of rotation of the magnetic field. Subsequently, A. Zibold [3] and A. Kapusta [4] proposed using a frequency-modulated rotating magnetic field (FM RMF) to increase the contribution of the turbulent component to the melt flow in order to increase the mixing efficiency.

Subsequently, L. Beitelman [5] proposed a method for improving macro- and microstructure of metal alloys by creating a superposition of two or more electromagnetic fields of different frequencies and/or amplitudes between multiple stirrers arranged in series.

Mikhailovich, Kapusta, and Levy [6] presented methods for optimizing heat and mass transfer using amplitude-frequency modulation (AFM), i.e., a combination of amplitude and frequency modulations, of TMF or RMF. Xiaodon et al. [7] proposed a solution for heat and mass transfer based on multidimensional numerical modeling.

Additional theoretical and experimental developments on using AFM for EMS were described by Dardik [8] and by Feldman [9]. These authors described how AFM RMF increases the turbulent component of melt flow, thereby reducing the time needed for stirring.

Varying parameters of the AFM inductor coil current affects the crystallization process and affects the macro- and microstructure of the continuously cast billets. However, the absence of criteria for optimizing the stirring process means that practitioners must test many AFM parameter combinations to find effective values, which is a significant cost and time burden.

SUMMARY

Embodiments of the present invention provide methods for increasing the stirring intensity of electromagnetic stirring (EMS), using resonant values for amplitude and frequency modulation. Applications include continuous and stationary melt casting of ferrous and non-ferrous metals, as well as out-of-furnace ladle casting. The invention is developed from an analysis of resonant phenomena arising from the interaction of AFM RMF or TMF with electrically conductive media.

Optimization of electromagnetic stirring parameters, in particular of a modulation frequency ω_f , is based on optimizing magnetic field vector potentials, given boundary conditions for different types of casting. Methods are provided for out-of-furnace processing of metals in ladle and for continuous or stationary billet casting. In the latter case, two options for the AFM RMF impact on the melt are considered: 1) creating conditions for electromagnetic forces resonance in the liquid core directly and 2) excitation of the electromagnetic forces causing resonance in the mold wall, which transfers the mechanical vibrations to the liquid core of the ingot. With the penetration of the AFM magnetic field into the wall of the mold, the Fourier amplitudes of the harmonic spectrum are reduced because of the skin effect. Part of this energy is converted into mechanical oscillations of the mold. Consequently, the following three force factors act on the liquid core of ingot: an average electromagnetic force,

exciting large-scale convection of the melt; resonance oscillations of the liquid core of the ingot; and additional mechanical vibrations of the melt, caused by mold vibration, through the solidified portion of ingot.

In some embodiments, a modulation frequency ω_f is chosen so that a frequency of amplitude modulation ω_a is equal to or is a multiple of one of the frequencies of harmonics of the Fourier spectrum Ω_n in the melt.

The maximum amplitude of electromagnetic forces, as represented by the vector potential, provides the high intensity of melt turbulence, suppressing the growth of dendrites and inclusions (clusters) and, thus promotes the fine-grained formation of solidified structure and chemical uniformity of billets, blooms and ingots.

BRIEF DESCRIPTION OF DRAWINGS

For a better understanding of various embodiments of the invention and to show how the same may be carried into effect, reference is made, by way of example, to the accompanying drawings. Structural details of the invention are shown to provide a fundamental understanding of the invention, the description, taken with the drawings, making apparent to those skilled in the art how the several forms of the invention may be embodied in practice. In the accompanying drawings:

Figs. 1 and 2 are schematic illustrations of a ladle for molten ingot casting;

Fig. 3 is a schematic illustration of a liquid core of square ingot section;

Fig. 4 is a schematic illustration of a wall mold with a square cross-section;

Fig. 5 is a schematic illustration of a liquid core of a circular ingot section;

Fig. 6 is a schematic illustration of a wall mold with circular cross-section; and

Fig. 7 is a schematic illustration of a dependence of the vector potential amplitude, in a melt, on the frequency of the driving inductive current.

DETAILED DESCRIPTION OF THE INVENTION

Hereinbelow, variables have the meanings indicated in the following table:

Variable	Description
ω_f	Ratio of frequency of modulation to the carrier frequency = $\frac{\omega_{fd}}{\omega_0}$ (i.e., "dimensionless modulation frequency")
ω_{fd}	Frequency of modulation, also referred to as f_{fd} (in Hz).
f_{fd}	Frequency of modulation, also referred to as ω_{fd} (in radians). f_{mres} is the modulation frequency at resonance
ω_a	Amplitude modulation frequency
$\bar{\omega}$	Dimensionless frequency of the EMF in the melt with specific electrical conductivity, σ_m , and with inner radius of the ladle R_0 and a melt level height Z_0 : $\bar{\omega} = \mu_0 \sigma_m \omega_0 R_0^2$
ξ	Frequency modulation index, $\xi = \Delta\omega / \omega_f$
$\Delta\omega$	Frequency deviation
Ω_n	Flow angular velocity of the n^{th} harmonic of the Fourier spectrum, $\Omega_n = (1 + n\omega_f) / \omega_0$
Ω	Flow angular velocity
$\langle \Omega \rangle$	Dimensionless vorticity of the turbulent melt motion velocity (\vec{V})
\vec{V}	Mean velocity vector of the turbulent liquid motion
ν	Melt kinematic viscosity

n	Number of frequencies in Fourier harmonic packet of the TMF, used to apply AFM
Re	Reynolds number = $\Omega R_0^2/\nu$
I	Current in each phase of inductor coils = $I_0(1 + \chi \sin \omega_a t) \sin(\omega_0 t + \xi \sin \omega_f t) =$ $I_0(1 + \chi \sin \omega_a t) \sum_{n=-\infty}^{\infty} J_n(\xi) \sin \Omega_n t$
I_0	Nominal current
\vec{a}	vector potential of magnetic field
$a_{z_Li_sq}, a_{z_Li_cyl}$	The z component of the dimensionless vector potentials of magnetic induction. For square and cylindrical ingots.
A_{nl}	Amplitude of the vector potential
δ	dimensionless wall thickness of the mold, defined as $\delta = \frac{\delta_d}{X_0}$
δ_d	the dimensional thickness of the mold wall
X_0	half-length of the outer mold side
$\Delta_{M_{sq}}$	penetration depth of magnetic field into the mold wall, $\Delta_{M_{sq}} = \sqrt{\frac{2}{\mu_0 \sigma_M \omega_0}}$
φ	Angle of inductor's working space (angle of coil around ladle, as indicated in Fig. 2)
$\bar{\varphi}$	dimensionless azimuthal coordinate of inductor working space = $\frac{\varphi}{2\pi}$
Z_0	Height of the liquid phase in active zone of ingot core.
z_d	dimensional axial coordinate of the melt
R_0	radius of the liquid phase in active zone of ingot core (liquid core size)

a_φ	azimuthal component of the vector potential
$\theta(\bar{\varphi})$	step function, equal to $\theta(\bar{\varphi}) = \begin{cases} 1, & -\bar{\varphi}_0 < \bar{\varphi} < \bar{\varphi}_0 \\ 0, & -\bar{\varphi}_0 > \bar{\varphi} > \bar{\varphi}_0 \end{cases}$
$\Phi^*(t)$	time function, which has the following form (in accordance with [10]) $\Phi^*(t) = (1 + \chi e^{-i\pi\omega_a t}) \sum_{n=-\infty}^{\infty} J_n(\xi) e^{i\pi\Omega_n t}$
$P_{kl} = \frac{\gamma_{kl}^2}{\bar{\omega}}$	dimensionless parameter used in expressions
$Q_1 = \frac{1}{\delta_z^2 \tau^2 \bar{\omega}}$	dimensionless parameter used in expressions
γ_{kl}	roots of the Bessel equation J_{ν_l} : $\left. \frac{\partial}{\partial r} J_{\nu_l}(\gamma_{kl} r) \right _{r=1} = 0,$
ν_l	$= \sqrt{1 - l^2}$
μ_0	magnetic permeability of a vacuum
δ_z	aspect ratio defined by equation $\delta_z = \frac{z_0}{2R_0}$
τ	pole division of an inductor

When a harmonic RMF of inductor coils interacts with a melt, a field of rotating currents is induced in the latter. Frequency of an induced magnetic field is equal to the frequency of the coil RMF current. The interaction of RMF and induced currents generates electromagnetic volumetric forces, which contain constant and variable components that change with double the frequency of the RMF.

Under the action of a constant force in the melt, a turbulent rotational flow arises. The flow structure in the liquid core is characterized by a quasi-solid core with a boundary layer on a liquid-solid phase transition area. The layer thickness depends on the Reynolds number, Re

$$Re = \Omega R_0^2 / \nu$$

where Ω is the angular flow velocity, R_0 is the liquid core radial size, and ν is the melt kinematic viscosity.

The variable component of the electromagnetic volumetric forces is partially suppressed by the walls of the crystallizer, if the inductor is located in the crystallizer, or on the crystallized ingot shell, if the inductor is located below the crystallizer. In both cases, the variable component of the electromagnetic volumetric forces stimulates the vibration of the walls of the crystallizer, or the surface of the solid phase of the ingot at a certain frequency.

Thus, the interaction of the RMF induction coils with the melt occurs in two opposite directions. On the one hand, the RMF supports the level of average stream velocity and turbulence generated by these streams. On the other hand, the RMF partially suppresses turbulence and transforms part of the turbulence energy into heat. Consequently, the stability of the state of the hydrodynamic system at a given RMF intensity is the result of these processes interaction.

Because the frequency of the inductor current is chosen from the condition of the maximum angular velocity in the melt, only the total inductor power is a parameter that affects the quality of the ingot. These power values reach 200 kVA and higher at existing plants.

However, increasing the inductor power by harmonic stirring method does not lead to a stirring intensity. The effect of the magnetic field on the melt velocity weakens with increasing intensity due to the asynchronous character of the electrodynamic processes. Simultaneously, the turbulent flow of the melt is suppressed by a strong magnetic field which leads to deterioration of heat and mass transfer intensity in the melt.

Limitations of the RMF stirring method led us to develop the method of resonant electromagnetic impact (REMI), based on optimization of AFM RMF parameters.

When the AFM RMF is generated in the inductor coils, the current amplitude in each phase can be represented by the following formula

$$I = I_0(1 + \chi \sin \omega_a t) \sin(\omega_0 t + \xi \sin \omega_f t) \quad (1)$$

where, I_0 is the nominal current,

ω_a is the amplitude modulation frequency,

ω_0 is the carrier frequency (frequency used in the plant),

ω_f is the frequency modulation frequency,

$\xi = \Delta\omega/\omega_f$ is the frequency modulation index,

$\Delta\omega$ is the frequency deviation.

As shown in [10], formula (1) can be represented in the form,

$$I = I_0(1 + \chi \sin \omega_a t) \sum_{n=-\infty}^{\infty} J_n(\xi) \sin \Omega_n t \quad (2)$$

where $\Omega_n = (1 + n\omega_f)/\omega_0$

As follows from formula (2), the AFM currents can be represented as a Fourier series in which there are frequency terms of higher and lower values than the carrier frequency. The carrier frequency is the operating frequency of the harmonic current used in the casting technology for a particular electromagnetic stirring setup.

A mathematical study of the Maxwell equation describing the electrodynamic processes in the liquid core of ingots of square and circular cross sections and in the wall of the corresponding crystallizer shows that resonant energy transfer occurs from one of the Fourier harmonics of the AFM RMF or TMF to the melt or to the copper wall of the crystallizer (i.e., the mold).

The resonance conditions are obtained as a result of solving a three-dimensional nonstationary equation for the vector potential \vec{a} :

$$L\vec{a} - \frac{\bar{\omega}}{\pi} \left(\frac{\partial \vec{a}}{\partial t} + \vec{V} \times \text{rot} \vec{a} \right) = 0 \quad (3)$$

where,

\vec{V} is the mean velocity vector of the turbulent liquid motion;

L is a vector operator, which is written as follows, depending on the spatial symmetry of the object. For a square ingot section, in a Cartesian coordinate system x, y, z :

$$L = \frac{\partial^2}{\partial x^2} + \frac{\partial^2}{\partial y^2} + \frac{\partial^2}{\partial z^2} \quad (4)$$

For a circular ingot section, or the ladle, in cylindrical coordinate system r, φ, z :

$$L = DD_* + \frac{1}{\pi r^2} \frac{\partial^2}{\partial \bar{\varphi}^2} + \frac{1}{\delta_Z^2} \frac{\partial^2}{\partial z^2} \quad (5)$$

where $D = \frac{\partial}{\partial r}$, $D_* = \frac{\partial}{\partial r} + \frac{1}{r}$, $\bar{\varphi} = \frac{\varphi}{2\pi}$, $\delta_Z = \frac{Z_0}{2R_0}$,

Z_0 and R_0 are the height and radius of the liquid phase in active zone respectively.

The active zone is determined as a height of an inductor pole. Boundary conditions for electromagnetic stirring for stirring in ladle or arc furnace and in square and circular section ingots are presented below.

Boundary conditions for different melt configurations

Boundary conditions for stirring in a ladle (Figs. 1 and 2):

Figs. 1 and 2 show a configuration of a typical metallurgical ladle mold **20**, having a mold wall **22**, to which is affixed an inductor **24**, for example, a traveling magnetic field (TMF) inductor. The inductor **24** has inductor poles **26**. Inside the mold is the melt **28** (typically a conductive metal liquid), and the slag **30**. As indicated, the conductive melt has a height Z_0 . Fig. 2 shows the mold from above, including the mold wall **22** and the inductor **24**. The mold radius is shown as R_0 .

$$\left. \frac{1}{r} \frac{\partial(r a_\varphi)}{\partial r} \right|_{r=R_0} = e^{-\frac{i\pi z}{\tau}} \theta(\bar{\varphi}) \Phi^*(t), \quad (6)$$

where a_φ is a component of the vector potential,

$\theta(\bar{\varphi})$ is a step function, equal to

$$\theta(\bar{\varphi}) = \begin{cases} 1, & -\bar{\varphi}_0 < \bar{\varphi} < \bar{\varphi}_0 \\ 0, & -\bar{\varphi}_0 > \bar{\varphi} > \bar{\varphi}_0 \end{cases}$$

$\Phi^*(t)$ is a time function, which has the following form accordance to [10]

$$\Phi^*(t) = (1 + \chi e^{-i\pi\omega_a t}) \sum_{n=-\infty}^{\infty} J_n(\xi) e^{i\pi\Omega_n t} \quad (7)$$

where $\bar{\varphi}_0$ is shown in **Fig. 2** as the working angle of the inductor element; χ is an amplitude depth modulation, Ω_n is non-dimensional angular frequency (i.e., velocity), J_n – Bessel

function of the first kind of order n , $\xi = \frac{\Delta\omega}{\omega_f}$ – frequency modulation index, $\Delta\omega$ – frequency deviation, ω_f – carrier frequency.

Boundary conditions for square ingot section (Figs. 3 and 4):

Figs. 3 and 4 show a configuration of a typical metallurgical square ingot mold **40**, in which is a melt **42** (also referred to hereinbelow as the liquid core), surrounding by a square mold wall **44**. (The inductor is not shown.) The width of the mold wall is shown as δ_d .

The boundary conditions are written in the Cartesian coordinate system.

Two variants of the AFM exposure on the ingot liquid core were considered:

a) Magnetic field of the inductor coils current affects directly to the liquid core of the ingot (Fig.2). The z - component of the dimensionless vector potential of magnetic induction a_{z_Liqsq} has the following form on the lateral surface of melt

$$a_{z_Liqsq} \Big|_{x=1} = (1 - iY)\Phi^*(t) \quad (8)$$

and in the mold center

$$a_{z_Liqsq} \Big|_{x=0} = 0 \quad (9)$$

b) Magnetic field of the inductor coils current acting on the liquid core through the vibration of the mold wall (Fig.3). The y - component of the vector potential a_{z_Msq} has the following form on the outer mold surface

$$a_{z_Msq} \Big|_{x=1} = -(1 - iY)\Phi^*(t), \quad (10)$$

and on the inner mold wall $x = 1 - \delta$

$$a_{z_Msq} \Big|_{x=1-\delta} = -(1 - iY)\Phi^*(t) * e^{-\frac{\delta_d}{\Delta Msq}} \quad (11)$$

where the dimensionless wall thickness of the mold δ is defined as $\delta = \frac{\delta_d}{X_0}$; δ_d is the dimensional thickness of the mold wall; X_0 is half of the dimensional outer mold side length,

$\Delta_{M_{sq}}$ – dimensional depth of magnetic field penetration into the mold wall is determined by

the following expression $\Delta_{M_{sq}} = \sqrt{\frac{2}{\mu_0 \sigma_M \omega_0}}$.

Boundary conditions for circular ingot section

Figs. 5 and 6 show a configuration of a typical metallurgical circular, or cylindrical ingot mold **60**, in which is a melt **62** (also referred to hereinbelow as the liquid core), surrounding by a cylindrical mold wall **64**. (The inductor is not shown.) The width of the mold wall is shown as δ_d . There are two variants of the AFM exposure on the ingot liquid core:

a) Magnetic field of the inductor coils current directly affects the liquid core of the ingot (Fig.4). z - component of the vector potential $a_{z_Liqlcycl}$ has following form on the external side surface of ingot

$$\left. \frac{\partial a_{z_Liqlcycl}}{\partial r} \right|_{r=1} = -e^{-i\pi\bar{\varphi}} \Phi^*(t), \quad (12)$$

and in the mold center $r = 0$

$$a_{z_Liqlcycl} \Big|_{r=0} = 0 \quad (13)$$

b) Magnetic field of the inductor coils current acts on the liquid core through the vibration of the mold wall (Fig.5). z - component of the scalar vector potential a_{z_Mcycl} has the following form on the outer mold surface $x = 1$ --

$$a_{z_Mcycl} \Big|_{r=1} = -e^{-i\pi\bar{\varphi}} \Phi^*(t), \quad (14)$$

on the inner mold wall $r = 1 - \delta$

$$a_{z_Mcycl} \Big|_{x=1-\delta} = a_{z_Mcycl} \Big|_{r=1} * e^{-\frac{\delta_d}{\Delta_{Mcycl}}} \quad (15)$$

where the dimensionless wall thickness of the mold δ is defined as $\delta = \frac{\delta_d}{X_0}$; δ_d is the dimensional thickness of the mold wall; X_0 is half-length of the outer mold side $\Delta_{M_{cyl}}$ - penetration length of magnetic field into the mold wall $\Delta_{M_{cyl}} = \sqrt{\frac{2}{\mu_0 \sigma_M \omega_0}}$.

The procedure of solving electrodynamic problems is common to all the above mentioned configurations and includes the following:

1. A double conversion of physical variables which change the form of original equations (1) with appropriate boundary conditions
2. Solving the obtained equations by the Galerkin method by expanding the initial function into a single or double series with respect to the space variables.
3. Obtaining an equation for determining time-dependent expansion coefficients. The solution of this equation and its investigation on the existence of extremums.
4. Obtaining formulas for the calculation of the value of resonance parameters.

Solutions for different configurations

Solving for resonance of the vector potential resonance for the boundary conditions of the different configurations gives formulas for calculating the resonance modulation frequencies for the different configurations. The amplitude ω_a and the frequency ω_f modulation are assumed below to be equal to each other, i.e., $\omega_a = \omega_f$

where,

ω_a amplitude modulation of the frequency is determined by the formula $\omega_a = \frac{2\pi f_a}{\omega_0}$,

f_a is the dimensional frequency of frequency modulation,

ω_0 is the dimensional frequency of carrier frequency.

Solutions are given for both the resonant mode of the liquid core and resonance of the vibration of the mold wall. Transitions from the resonant mode of the liquid core to the vibration of the mold wall may be performed by setting a duty cycle for the transition.

1. Cylindrical Ladle

$$\omega_f = (P_{kl} + Q + \Omega_0 - 1)/(n + 1),$$

where,

$$\omega_f = \frac{\omega_{fd}}{\omega_0}, \quad \omega_{fd} \text{ is a frequency of modulation,}$$

n is a number of Fourier harmonic oscillations in a packet of a traveling magnetic field (TMF) caused by an amplitude-frequency modulation of a TMF inductor;

$$P_k = \frac{\gamma_k^2}{\bar{\omega}},$$

γ_k are the roots of equation $D^* J_{\kappa}(\gamma_k) = 0$, where $J_{\kappa}(\gamma_k)$ is a Bessel function,

$$\kappa = \sqrt{1 + l^2}, \quad k, l = 1, 2, 3 \dots$$

$$Q = \frac{\pi^2}{\delta_z^2 \tau^2 \bar{\omega}},$$

$$\bar{\omega} = \mu_0 \sigma \omega_0 R_0^2,$$

$$\Omega_0 = \nu \cdot 10^5 / R_0 \omega_0, \quad \text{estimated melt angular velocity,}$$

ω_0 is the carrier angular frequency,

ν is the melt kinematic viscosity,

$$\delta_z = \frac{Z_0}{2R_0}, \quad \text{is a normalized melt height,}$$

Z_0, R_0 are ladle height and radius,

σ specific electrical conductivity,

μ_0 is the magnetic permeability of a vacuum,

τ is a pole division of an inductor.

2. Square mold – core mixing

$$\omega_f = (1 - \Omega_n)/(n + 1),$$

where,

$$\Omega_n = \frac{P_{kl}^2}{P_{kl} + \Omega_0} \left(\sqrt{\left(\frac{P_{kl} + \Omega_0}{P_{kl}} \right)^2 + 1} - 1 \right),$$

$$P_{kl} = \pi^2 (k^2 + l^2) / \bar{\omega},$$

$$\bar{\omega} = \mu_0 \sigma \omega_0 X_0^2,$$

$$k, l = 1, 2, 3 \dots,$$

σ is the specific electrical conductivity of the melt, and

X_0 is a half of the billet cross-section length size.

3. Square ingot – wall vibration

$$\omega_f = (0.414 P_{kl} - 1)/(n + 1),$$

where,

$$P_{kl} = \pi^2 \left(\frac{k^2}{\delta^2} + \frac{l^2}{(2-\delta)^2} \right) / \bar{\omega},$$

$\bar{\omega} = \mu_0 \sigma_{Co} \omega_0 X_0^2$, where σ_{Co} is electrical conductivity (of copper),

$k, l = 1, 2, 3 \dots$

$\delta = \delta_m / X_0$ is a dimensionless mold wall thickness,

δ_m is the dimensional mold wall thickness,

X_0 is the half length of the outer mold cross-section side length.

4. Cylindrical ingot – core mixing

$$\omega_f = (1 - P_k + \Omega_0) / (n + 1),$$

where,

$$P_k = \frac{1}{\bar{\omega}_{Liq\,cir}} \beta_k^2,$$

where the relative melt frequency $\bar{\omega}$ is determined by the formula $\bar{\omega} = \mu_0 \sigma_{Liq} \omega_0 R_{Liq}^2$;

σ_{Liq} is a the specific electrical conductivity of the melt,

R_{Liq} is the internal radius of the mold cross-section,

β_k are the roots of the equation $\frac{\partial}{\partial r} J_1(\beta_k r) \Big|_{r=1} = 0$,

r is the liquid core radius of the melt,

Ω_0 is the dimensionless angular velocity of the melt (turbulent melt motion) defined

$$\text{by: } \Omega_0 = \frac{Q_0}{2} \left(\sqrt{1 + \frac{4}{Q_0}} - 1 \right),$$

$$Q_0 = \frac{Ha^2 \delta_z}{0.0487 Re_\omega},$$

$Ha = B_0 R_0 \sqrt{\frac{\sigma}{\eta}}$ is the Hartman number,

B_0 is a magnetic induction in inductor core,

$$Re_\omega = \frac{\omega_0 R_0^2 \rho}{\eta} \sigma,$$

σ and η are the electrical conductivity and dynamic viscosity of the melt,

ρ is a melt density,

$$Re_\omega = \frac{R_0^2 \omega_0}{\nu}$$

$k=1, 2, 3 \dots$

5. Cylindrical mold – wall vibration

$$\omega_f = (1 - P_k)/(n - 1),$$

where,

$$n = 1, 2, 3 \dots;$$

$$P_k = \frac{\zeta_k^2}{\bar{\omega}}, \bar{\omega} = \mu_0 \sigma \omega_0 R_0^2,$$

ζ_k are the roots of equation:

$$\frac{\partial}{\partial r} J_1[\zeta_k(1 - \delta)] \cdot \frac{\partial}{\partial r} Y_1(\zeta_k) - \frac{\partial}{\partial r} J_1(\zeta_k) \cdot \frac{\partial}{\partial r} Y_1[\zeta_k(1 - \delta)] = 0,$$

where $\frac{\partial J_1}{\partial r}$ is a derivative of the first kind Bessel function of the first order,

$\frac{\partial Y_1}{\partial r}$ is a derivative of the second kind Bessel function of the first order, and

$k, l = 1, 2, 3 \dots$

Examples of implementation

The electromagnetic force volume \vec{f} equals the vectorial multiplication of real components of the current density $Re\vec{j}$ and the magnetic induction $Re\vec{b}$

$$\vec{f} = Re\vec{j} \times Re\vec{b}$$

The current density \vec{j} and the magnetic induction \vec{b} are proportional to the A_{nl} , the amplitude of the vector potential \vec{a} , which is also proportional to the motion velocity of the melt, \vec{V} . Consequently, resonant amplitudes of the vector potential and the variable component of electromagnetic volume forces \vec{f} are proportional (though the frequency of change of the field of forces is equal to double the vector potential frequency). The dependence of the vector potential amplitude A_{nl} on the frequency modulation Ω_n of the TMF or RMF also characterizes changes in the electromagnetic volume force \vec{f} .

Fig. 7 shows a graph **100** of A_{nl} vs. Ω_n for an exemplary melt configuration. The maximum value of A_{nl} indicates the optimal modulation harmonic Ω_n , from which to derive the optimal modulation frequency ω_{fd} or f_{mres} (i.e., the "resonance" frequency of modulation).

Example 1: Steel Ingot

$$\omega_f = (1 - \Omega_n)/(n + 1)$$

$$\Omega_n = \frac{P_{kl}^2}{P_{kl} + \Omega_0} \left(\sqrt{\left(\frac{P_{kl} + \Omega_0}{P_{kl}} \right)^2 + 1} - 1 \right),$$

$$P_{kl} = \pi^2(k^2 + l^2)/\bar{\omega}, \bar{\omega} = \mu_0 \sigma_{melt} \omega_0 X_0^2, k, l = 1, 2, 3 \dots$$

Steel ingot is a square cross section 300x300mm,

copper mold wall thickness of 12mm,

$$\delta = 0.074,$$

$$\omega_0 = 314 \text{ rad/s.}$$

The frequency of the resonant Fourier harmonic is determined by the following formula

$$\Omega_{nres} = 0.41 * P_{kl}$$

$$\text{where } P_{kl} = \pi^2 \left[\frac{k^2}{\delta^2} + \frac{l^2}{(2-\delta)^2} \right] \frac{1}{\bar{\omega}};$$

$$\bar{\omega} = \mu_0 \sigma_M \omega_0 X_0^2 = 279.5.$$

At k=1, l=1 Therefore, at k=1, l=1 we obtain

$$P_{kl} = 6.45; \Omega_{nres} = 2.67; \omega_f = 0.56;$$

Fourier harmonic, n = 1 and modulation frequency of f_{mres} is equal to

$$f_{mres} = \omega_f * \omega_0 = 27.8 \text{ Hz}$$

Example 2: Steel ingot is a circular cross section

Diameter 300mm. The frequency of the resonant Fourier harmonic is determined by the following formula

$$\Omega_{nres} = \sqrt{P_k^2 - \Omega^2}, \Omega = 0.1,$$

where,

$P_k = \frac{\gamma_k^2}{\bar{\omega}}$; $Y_1 = 1.8412$; $\bar{\omega} = \mu_0 \sigma \omega_0 R_0^2 = 0.64$, $\omega_0 = 31.4 \text{ rad/s}$. Therefore, at $k=1$, $l=1$ $P_{kl} = 5.3$; $\Omega_{nres} = 5.3$; $\omega_f = 0.86$; Fourier harmonic number $n = 4$ and dimensional modulation frequency of f_{mres} is equal to

$$f_{mres} = \omega_f * \omega_0 = 4.3 \text{ Hz}$$

As follows from the boundary conditions (6 - 14), the AFM TMF or RMF is excited by means of superposition of two nonlinear rotating magnetic fields, when one of them is frequency-modulated and the other one is amplitude modulated. Formally, resonance frequencies Ω_n are equal for each field. However, the frequency spectra for the same Ω_n are different, since the carrier frequencies of the nearest neighboring harmonics differ by the magnitude amplitude modulation ω_a .

Due to the processes of dissipation in the melt or in the mold, the resonance curves in all the considered cases smoothly change near the resonance (Fig. 6). Thus, a large number of Fourier harmonics have amplitude close to the resonant amplitude, which ensures the stability of turbulent flows and a high intensity of heat and mass transfer.

In practical application of REMI method, the frequency modulation of the frequency ω_f is chosen so that the harmonics ω_a will be equal to one of the frequency of spectrum Ω_n .

The condition defining of amplitude modulation ω_a for the positive value n , has a following form

$$\omega_{f-res} = \frac{\omega_a}{n_1 - n_2} \quad (16)$$

If the module $|n_1 - n_2| = 1$,

$$\omega_{a-res} = \omega_{f-res} \quad (17)$$

The REMI method initiates the resonance of electromagnetic oscillations processes in the melt and crystallizer and creates the conditions for its maintenance. The excitation of nonlinear oscillations in the cross section of the liquid core or the mold wall is the energy source of the forced nonlinear waves propagating along the axis of the ingot. This effect is an additional factor to maintain the turbulent nature of the flow in those areas of the liquid core

of the ingot, where convection currents are weak or absent. Due to nonlinearity and the presence of rotational flow, waves propagating along the axis of the ingot transfer kinetic energy, strengthening heat and mass transfer to the crystallization front and along the liquid core. This should have a positive effect on reducing temperature and concentration gradients throughout the melt volume and, as a result, on the chemical and structural homogeneity of the final products.

The application of this method in electromagnetic stirring processes can effect: reduction in power consumption, more uniform temperature distribution in the melt, more uniform chemical distribution in the melt, reduction of the axial porosity of the ingot, an increase in the proportion of crystals in the ingot cross section, and improved quality of the ingot surface.

REFERENCES

1. E. Pestel et al., "Production of Fine Grained Metal Castings," U.S. Pat. No. 2963758, 1960.
2. S. Junghans, O. Schaaber, "Casting processes, in particular continuous casting method and Plant," Patent of Federal Republic of Germany, 1954, No. DE911425C.
3. A. Zibold et al. Author certificate N 1208888, USSR, 1984.
4. A. Kapusta et al. Author certificate N 1577452, USSR, 1985.
5. L. Beitelman et al. Modulated electromagnetic stirring of metals at advanced stage of solidification. EP 2268431 A4, Jul 12, 2017.
6. B. Mikhailovich, A. Kapusta, A. Levy, Proc. of EPM 2015, <https://hal.archives-ouvertes.fr/hal-01333913>.
7. W. Xiaodon et al, International Journal of Energy and Environmental Engineering, 6 (2015) 367–373.
8. Dardik I., et al. "Systems and methods of electromagnetic influence on electroconducting continuum," US Patent 7,350,559, April 1, 2008.
9. M. Feldman et al, AISTech - Iron and Steel Technology Conference Proceedings, 2 (2016) 1473-1481.

10. A. Angot, Compléments de Mathématiques à l'Usage des Ingénieurs de l'électrotechnique et des télécommunications. Paris, 1957.

CLAIMS

1. A method for optimizing electromagnetic stirring of a melt of electrically conductive fluids, comprising applying a modulation frequency ω_f to a carrier frequency ω_0 of an inductive current applied by an inductor to the melt, wherein the modulation frequency ω_f maximizes one or more of: an electromagnetic volume force \vec{f} , a current density \vec{j} , a magnetic induction \vec{b} , a motion velocity, \vec{V} , and an amplitude of vector potential, A_{nl} , of the melt, or of a mold wall of the melt.

2. The method according to claim 1, wherein the modulation frequency ω_f for the melt in a cylindrical ladle configuration is calculated as: $\omega_f = (P_{kl} + Q + \Omega_0 - 1)/(n + 1)$,

wherein,

$$\omega_f = \frac{\omega_{fd}}{\omega_0}, \quad \omega_{fd} \text{ is a frequency of modulation,}$$

n is a number of Fourier harmonic oscillations in a packet of a traveling magnetic field (TMF) caused by an amplitude-frequency modulation of a TMF inductor;

$$P_k = \frac{\gamma_k^2}{\bar{\omega}},$$

γ_k are the roots of equation $D^* J_\kappa(\gamma_k) = 0$, where $J_\kappa(\gamma_k)$ is a Bessel function,

$$\kappa = \sqrt{1 + l^2}, \quad k, l = 1, 2, 3 \dots$$

$$Q = \frac{\pi^2}{\delta_z^2 \tau^2 \bar{\omega}},$$

$$\bar{\omega} = \mu_0 \sigma \omega_0 R_0^2,$$

$$\Omega_0 = \nu \cdot 10^5 / R_0 \omega_0, \text{ estimated melt angular velocity,}$$

ω_0 is the carrier angular frequency,

ν is the melt kinematic viscosity,

$$\delta_z = \frac{Z_0}{2R_0}, \text{ is a normalized melt height,}$$

Z_0, R_0 are ladle height and radius,

σ specific electrical conductivity,

μ_0 is the magnetic permeability of a vacuum,

τ is a pole division of an inductor.

3. The method according to claim 1, wherein the modulation frequency ω_f for continuous or stationary ingots cast in a **square cross-section** mold is calculated as

$$\omega_f = \frac{1}{n+1} (1 - \Omega_n),$$

wherein angular velocity of the RMF Ω_n is defined as

$$\Omega_n = \frac{P_{kl}^2}{P_{kl} + \Omega_0} \left[\sqrt{\left(\frac{P_{kl} + \Omega_0}{P_{kl}} \right)^2 + 1} - 1 \right],$$

and wherein,

$n = 1, 2, 3 \dots$ is a Fourier harmonic number;

$$P_{kl} = [k^2 + l^2] \frac{\pi^2}{\bar{\omega}},$$

$k = 0, 1, 2 \dots, l = 1, 2, 3, \dots,$

$\bar{\omega}_{Liqsq} = \mu_0 \sigma \omega_0 X_{Liq}^2$ is a dimensionless frequency of EMF oscillations in the melt, created by an amplitude-frequency modulation of an RMF inductor,

σ is the specific electrical conductivity of the melt, and

X_0 is a half of the billet cross-section length size.

4. The method according to claim 1, wherein the modulation frequency ω_f for a **vibration of a square cross-section mold wall** for continuous or stationary casting is calculated as

$$\omega_f = (0.414 P_{kl} - 1) / (n + 1),$$

wherein,

$$P_{kl} = \pi^2 \left(\frac{k^2}{\delta^2} + \frac{l^2}{(2-\delta)^2} \right) / \bar{\omega},$$

$\bar{\omega} = \mu_0 \sigma_{Co} \omega_0 X_0^2$, where σ_{Co} is electrical conductivity (of copper),

$k, l = 1, 2, 3 \dots,$

$\delta = \delta_m / X_0$ is a dimensionless mold wall thickness,

δ_m is the dimensional mold wall thickness, and

X_0 is the half length of the outer mold cross-section side length.

5. The method according to claim 1, wherein the resonant modulation frequency ω_f for continuous or stationary ingots casting with a **circular** cross-section, is calculated as

$$\omega_f = \frac{1}{n+1}(1 - P_k + \Omega_0),$$

wherein,

$$n = 1, 2, 3 \dots,$$

$$P_k \text{ is defined as } P_k = \frac{1}{\bar{\omega}_{Liq\,cir}} \beta_k^2,$$

$$\bar{\omega} \text{ is determined by the formula } \bar{\omega} = \mu_0 \sigma_{Liq} \omega_0 R_{Liq}^2,$$

σ_{Liq} is a the specific electrical conductivity of the melt,

R_{Liq} - internal radius of the mold cross-section,

and β_k are the roots of equation

$$\left. \frac{\partial}{\partial r} J_1(\beta_k r) \right|_{r=1} = 0,$$

where r is the liquid core radius of the melt,

Ω_0 is the dimensionless angular velocity of the melt defined as

$$\Omega_0 = \frac{Q_0}{2} \left(\sqrt{1 + \frac{4}{Q_0}} - 1 \right),$$

$$Q_0 = \frac{Ha^2 \delta_z}{0.0487 Re_\omega},$$

$$Ha = B_0 R_0 \sqrt{\frac{\sigma}{\eta}} \text{ is the Hartman number,}$$

B_0 is a magnetic induction in inductor core,

$$Re_\omega = \frac{\omega_0 R_0^2 \rho}{\eta} \sigma,$$

σ and η are the electrical conductivity and dynamic viscosity of the melt, and

ρ is a melt density,

6. The method according to claim 5 for stimulating vibration of a **cylindrical mold wall** under the action of electromagnetic forces with a resonance dimensionless frequency of the frequency modulation ω_f , which is determined by the following formula

$$\omega_f = \frac{1}{n+1}(1 - P_k),$$

wherein,

$$n = 1, 2, 3 \dots; P_k \text{ is determined as}$$

$$P_k = \frac{\zeta_k^2}{\bar{\omega}},$$

$$\bar{\omega} = \mu_0 \sigma \omega_0 R_0^2,$$

σ is the specific electrical conductivity of the mold wall,

R_0 is an external radius of the mold cross-section,

ζ_k are the roots of equation: $\frac{\partial}{\partial r} J_1[\zeta_k(1 - \delta)] \cdot \frac{\partial}{\partial r} Y_1(\zeta_k) - \frac{\partial}{\partial r} J_1(\zeta_k) \cdot \frac{\partial}{\partial r} Y_1[\zeta_k(1 - \delta)] = 0$,

$\frac{\partial J_1}{\partial r}$ is a derivative of the first kind Bessel function of the first order, and

$\frac{\partial Y_1}{\partial r}$ is a derivative of the second kind Bessel function of the first order.

7. The method of claims 1 - 6, wherein frequencies of amplitude modulation ω_a and the frequency modulation ω_f are equal to each other ($\omega_a = \omega_f = \frac{2\pi f_{fd}}{\omega_0}$, f_{fd} is a frequency of modulation).
8. The method according to claims 3 and 4, wherein the transition from the resonant mode of the liquid core to the vibration of the mold wall with the required duty cycle is performed.
9. The method according to claims 5 and 6 wherein the transition from the resonant mode of the liquid core to the vibration of the mold wall with the required duty cycle is performed.

1/4

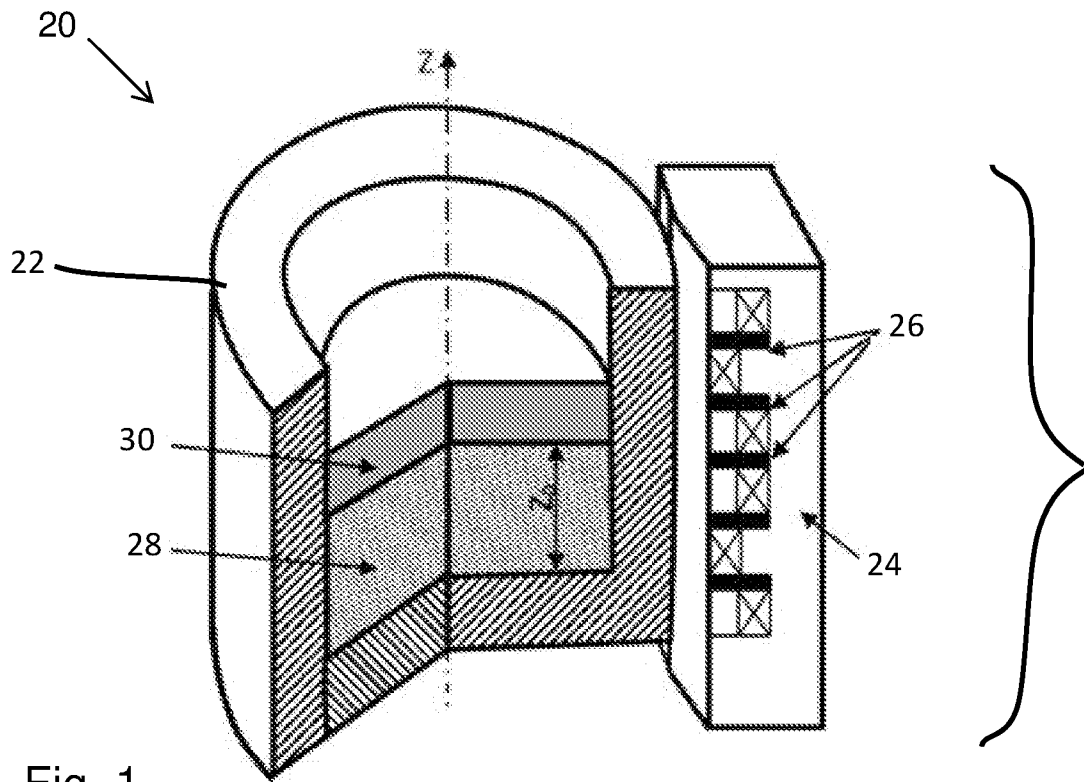


Fig. 1

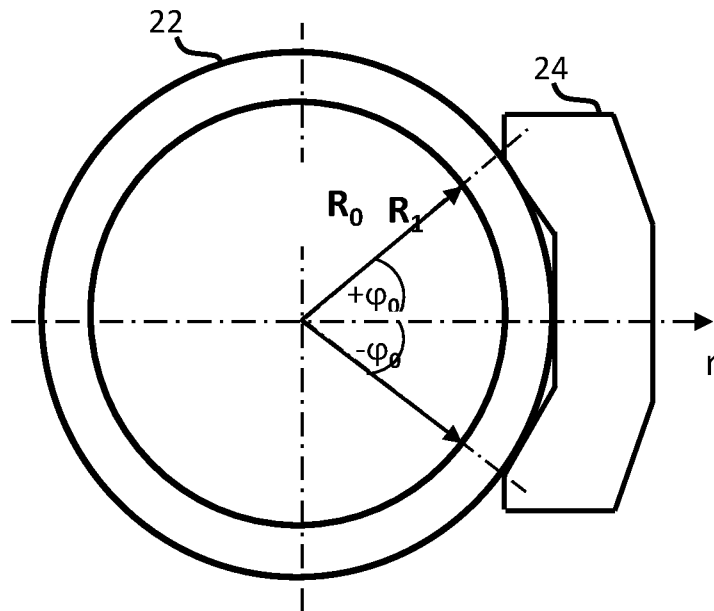


Fig. 2

2/4

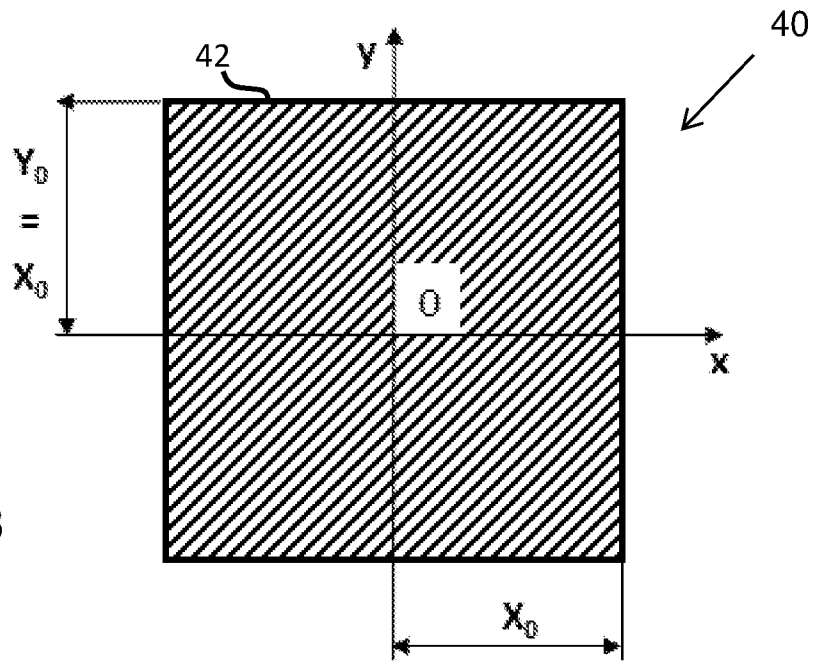


Fig. 3

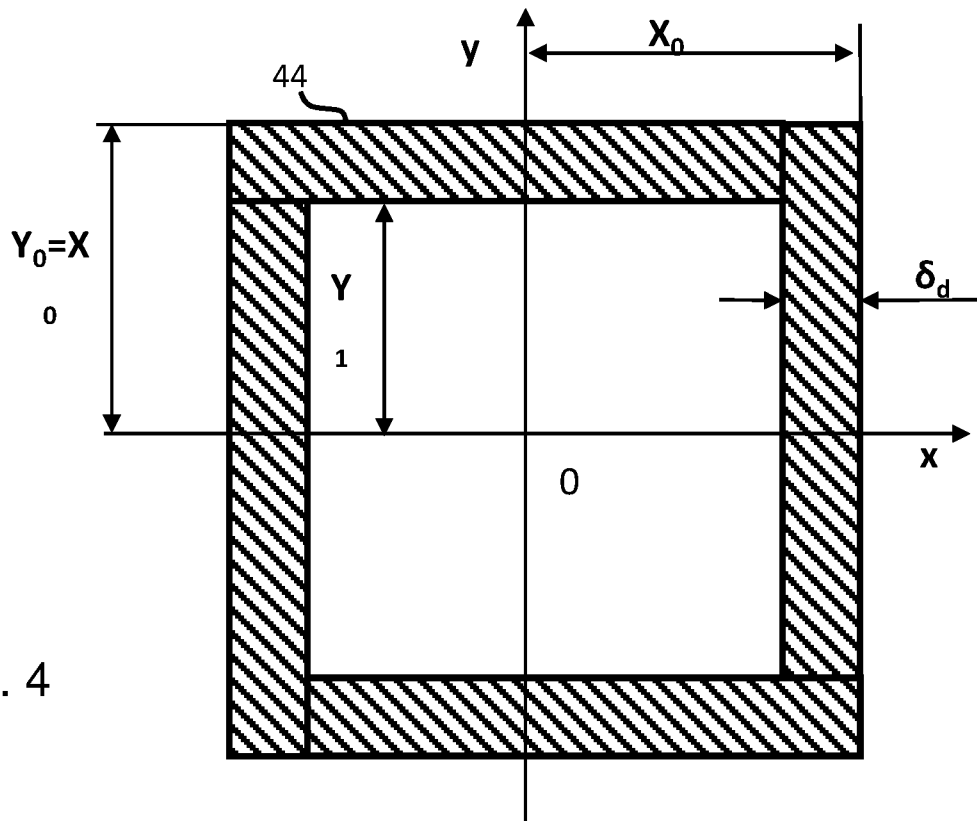


Fig. 4

3/4

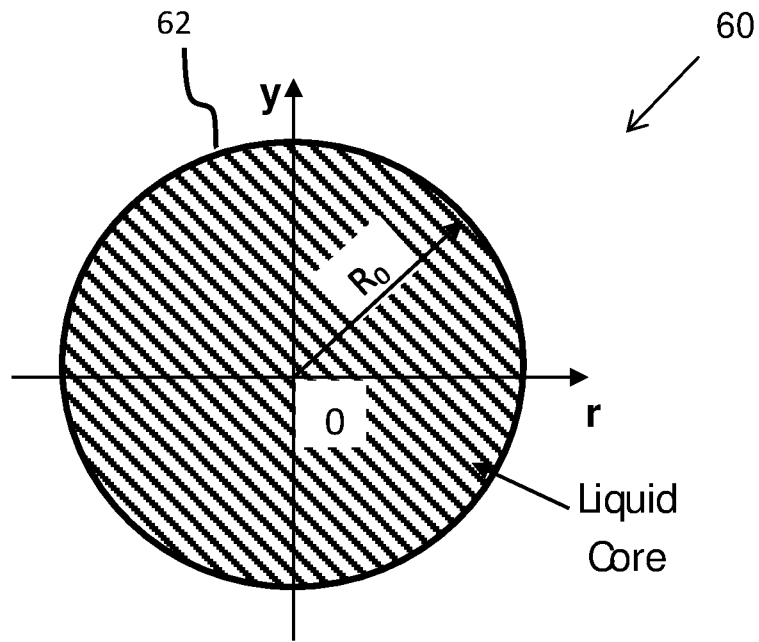


Fig. 5

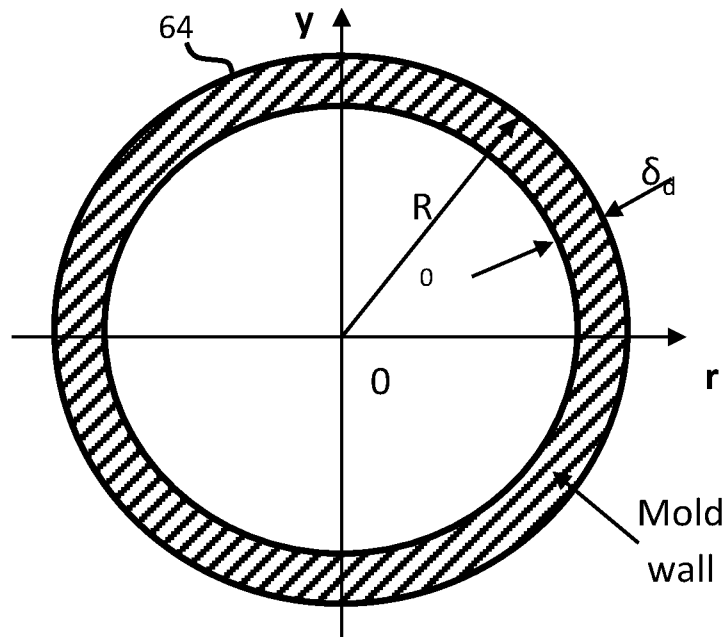


Fig. 6

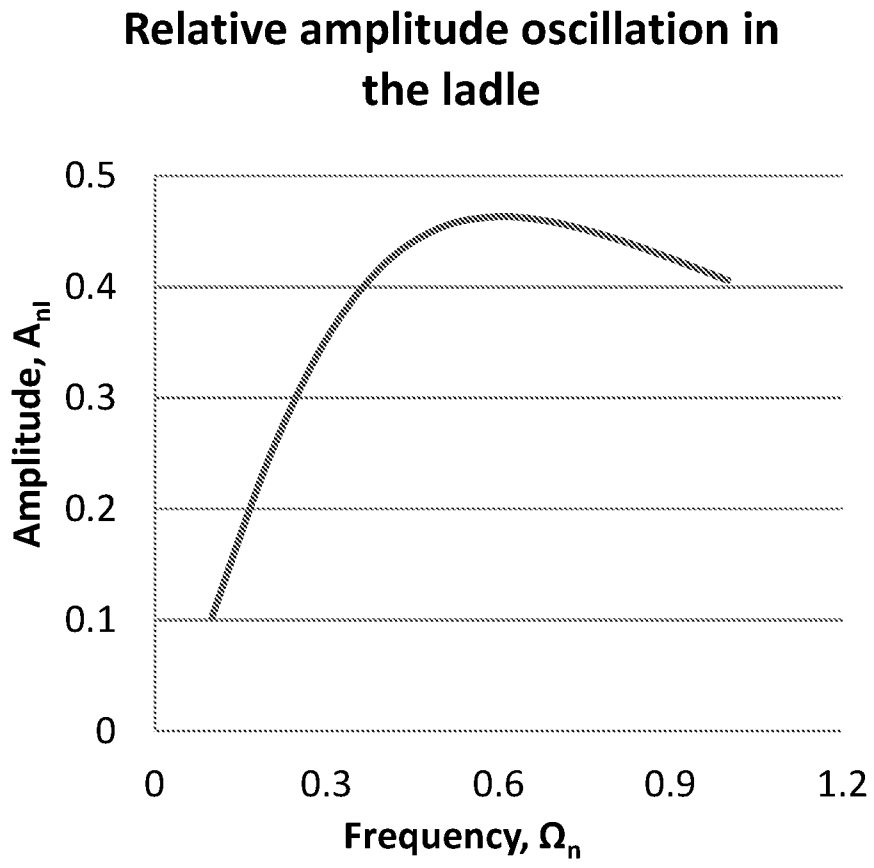
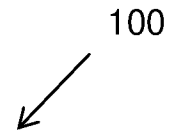


Fig. 7

INTERNATIONAL SEARCH REPORT

International application No
PCT/IL2019/050291

A. CLASSIFICATION OF SUBJECT MATTER
 INV. B22D11/115 B01F13/08 B22D11/12 B22D27/02 F27D27/00
 ADD.
 According to International Patent Classification (IPC) or to both national classification and IPC

B. FIELDS SEARCHED
 Minimum documentation searched (classification system followed by classification symbols)
 B22D B01F F27D

Documentation searched other than minimum documentation to the extent that such documents are included in the fields searched

Electronic data base consulted during the international search (name of data base and, where practicable, search terms used)
 EPO-Internal, WPI Data

C. DOCUMENTS CONSIDERED TO BE RELEVANT

Category*	Citation of document, with indication, where appropriate, of the relevant passages	Relevant to claim No.
X	US 2009/242165 A1 (BEITELMAN LEONID S [CA] ET AL) 1 October 2009 (2009-10-01) paragraph [0007] paragraph [0045] - paragraph [0047] paragraph [0052] paragraph [0001] paragraph [0009] - paragraph [0010] -----	1-9
X	FR 3 051 698 A1 (CONSTELLIUM ISSOIRE [FR]) 1 December 2017 (2017-12-01) page 5, line 18 - page 6, line 6 page 13, line 22 - page 14, line 30 -----	1-9
X	US 5 699 850 A (BEITELMAN LEONID [CA] ET AL) 23 December 1997 (1997-12-23) column 4, line 21 - column 5, line 16 ----- -/--	1-9

Further documents are listed in the continuation of Box C.

See patent family annex.

* Special categories of cited documents :

"A" document defining the general state of the art which is not considered to be of particular relevance	"T" later document published after the international filing date or priority date and not in conflict with the application but cited to understand the principle or theory underlying the invention
"E" earlier application or patent but published on or after the international filing date	"X" document of particular relevance; the claimed invention cannot be considered novel or cannot be considered to involve an inventive step when the document is taken alone
"L" document which may throw doubts on priority claim(s) or which is cited to establish the publication date of another citation or other special reason (as specified)	"Y" document of particular relevance; the claimed invention cannot be considered to involve an inventive step when the document is combined with one or more other such documents, such combination being obvious to a person skilled in the art
"O" document referring to an oral disclosure, use, exhibition or other means	"&" document member of the same patent family
"P" document published prior to the international filing date but later than the priority date claimed	

Date of the actual completion of the international search 24 April 2019	Date of mailing of the international search report 06/05/2019
--	--

Name and mailing address of the ISA/ European Patent Office, P.B. 5818 Patentlaan 2 NL - 2280 HV Rijswijk Tel. (+31-70) 340-2040, Fax: (+31-70) 340-3016	Authorized officer Desvignes, Rémi
--	---

INTERNATIONAL SEARCH REPORT

International application No
PCT/IL2019/050291

C(Continuation). DOCUMENTS CONSIDERED TO BE RELEVANT		
Category*	Citation of document, with indication, where appropriate, of the relevant passages	Relevant to claim No.
X	<p>WO 03/106009 A1 (COMMISSARIAT ENERGIE ATOMIQUE [FR]; BOEN ROGER [FR] ET AL.) 24 December 2003 (2003-12-24) page 3, line 20 - page 4, line 2 page 5, line 6 - line 22 page 10, line 2 - line 7 -----</p>	1-9
X	<p>Jacqueline Etay ET AL: "INSTITUT NATIONAL POLYTECHNIQUE DE GRENOBLE", 4 December 2002 (2002-12-04), XP055582987, Retrieved from the Internet: URL:https://hal.archives-ouvertes.fr/tel-01338830 [retrieved on 2019-04-24] page 89, paragraph 3.6 -----</p>	1-9
X	<p>B Mikhailovich ET AL: "Excitation of Oscillations in the Melt by Frequency-Modulated TMF", 12 October 2015 (2015-10-12), XP055583008, Retrieved from the Internet: URL:https://hal.archives-ouvertes.fr/hal-01333913/ [retrieved on 2019-04-24] page 2, paragraph Introduction -----</p>	1-9

INTERNATIONAL SEARCH REPORT

Information on patent family members

International application No PCT/IL2019/050291

Patent document cited in search report	Publication date	Patent family member(s)	Publication date
US 2009242165	A1	01-10-2009	AR 071042 A1 19-05-2010
			BR PI0822471 A2 16-06-2015
			CA 2719299 A1 01-10-2009
			CN 101980808 A 23-02-2011
			EP 2268431 A1 05-01-2011
			JP 2011515225 A 19-05-2011
			KR 20100139059 A 31-12-2010
			RU 2010143386 A 27-04-2012
			UA 102094 C2 10-06-2013
			US 2009242165 A1 01-10-2009
			WO 2009117803 A1 01-10-2009
FR 3051698	A1	01-12-2017	CA 3024166 A1 07-12-2017
			CN 109311081 A 05-02-2019
			EP 3463716 A1 10-04-2019
			FR 3051698 A1 01-12-2017
			WO 2017207886 A1 07-12-2017
US 5699850	A	23-12-1997	NONE
WO 03106009	A1	24-12-2003	FR 2840821 A1 19-12-2003
			GB 2408699 A 08-06-2005
			JP 4434946 B2 17-03-2010
			JP 2005534467 A 17-11-2005
			US 2005200442 A1 15-09-2005
			WO 03106009 A1 24-12-2003